Response of unconfined vortex breakdown to axial pulsing

Sammy Khalil,[a] Kerry Hourigan,[b] and Mark C. Thompson[c]
Fluids Laboratory for Aeronautical and Industrial Research (FLAIR)
Department of Mechanical Engineering, Monash University, Melbourne, 3800, Australia

(Received 19 October 2005; accepted 21 January 2006; published online 6 March 2006)

The response of unconfined swirling jets undergoing vortex breakdown to axial pulsing is explored experimentally. In particular, the combination of particle visualization and particle image velocimetry has enabled the effect of axial pulsing on the development of shear-layer flow structures and vortex breakdown to be quantified, as a function of both pulsing frequency and amplitude. A range of Reynolds and swirl numbers is considered. A key result is that application of low-level forcing at the natural frequency intensifies the shear-layer vortices considerably and results in a substantial relative downstream shift of the mean breakdown position. © *2006 American Institute of Physics*. [DOI: 10.1063/1.2180290]

Experimental research into vortex breakdown and vortex breakdown control techniques has been undertaken for the past 50 and 40 years, respectively (e.g., see Delery[1] and Lucca-Negro and O'Doherty[2]). The importance of understanding this phenomenon, and how to control it, is of considerable importance for applications such as heat exchangers and combustion control, but none more pronounced than in the aeronautical industry.

Controlling vortex breakdown near delta wings by introducing well-defined perturbations into the flow field though unsteady blowing has been used previously with success.[3–6] The most effective positions to implement control mechanisms are those close to the point of vortex conception and downstream of breakdown; however, in practice, the optimum practical control location is often upstream of breakdown. Although both continuous and pulsed blowing or suction causes a delay in the formation of the breakdown structure, there are certain advantages displayed by the pulsed approach; the most effective was found to be alternating blowing and suction.[6–9] It was shown[10] that pulsed blowing parallel to the leading edge was almost twice as effective in delaying vortex breakdown as continuous blowing.

In this Brief Communication, unsteady axial pulsing is investigated as a means to control breakdown of an effectively unconfined vortex core. An examination of the resulting breakdown structure and its movement, both locally and globally, was carried out. The primary aim of this investigation was to quantitatively record which frequencies and amplitudes of axial pulsing create the greatest movement of the vortex-breakdown (upstream) stagnation point, and to quantify the effect.

The swirling flows generated in this experiment were created by a method similar to that used by Billant *et al.*[11] and Wu *et al.*,[12] and consisted of a pressure-driven swirling water jet discharging into a large tank. The swirl is imparted by means of an electric servomotor, which rotates a honeycomb within a settling chamber. A schematic of the apparatus is shown in Fig. 1.

A laminar pulseless disk pump, creating a closed circuit with accurate control of axial flow rates, generates a smooth axial velocity. It also enables a more realistic simulation of a pulsing mechanism, which could be used in combustion chambers or in flight. Pulsing is achieved via an inline computer-controlled proportional-lift solenoid valve. Previous studies[3] have examined steady and unsteady suction and blowing of separate flows, which join the vortical structure somewhere along its path to control vortex breakdown. This experiment is novel in that it pulses the actual vortical structure in the axial direction at the point of generation. The flow rate, which in turn determines the axial Reynolds number, is controlled to within ±1% by a frequency inverter connected to the disk pump and an electronic flow meter. An azimuthal velocity component is imparted to the flow via a vortex generator. This consists of a motor and two concentric cylinders, similar to that used by Billant *et al.*[11] The fluid in the outer cylinder passes through the upper part of the inner cylinder through an arrangement of holes. In order to set the flow into laminar solid-body rotation (i.e., a Rankine vortex), the flow is then passed through a honeycomb located in the lower part of the rotating inner cylinder. The swirling jet then passes through a smooth converging nozzle, which is attached to the outer cylinder and is fixed, i.e., nonrotating. In order to avoid flow separation, the contraction zone is designed according to an optimum contraction design method.[13] The exit diameter of the contraction zone is $D=2R=39.5$ mm, where R is the jet radius. The nozzle was computer machined to an accuracy of better than 1%. A frequency inverter and servomotor control the frequency of rotation to within ±0.5%.

The vortex generator is partly submerged in a square cross section ($650\times650\times1500$ mm) transparent Perspex tank into which the swirling jet is discharged. Such a configuration allows the simulation of an almost unconfined vortex due to the large ratio of tank to jet area ($\simeq345$).

An intercooler setup was also incorporated to ensure minimal temperature gradients within the tank to avoid thermal convection currents. The intercooler involved passing

[a]Electronic mail: sammy.khalil@eng.monash.edu.au
[b]Electronic mail: kerry.hourigan@eng.monash.edu.au
[c]Electronic mail: mark.thompson@eng.monash.edu.au

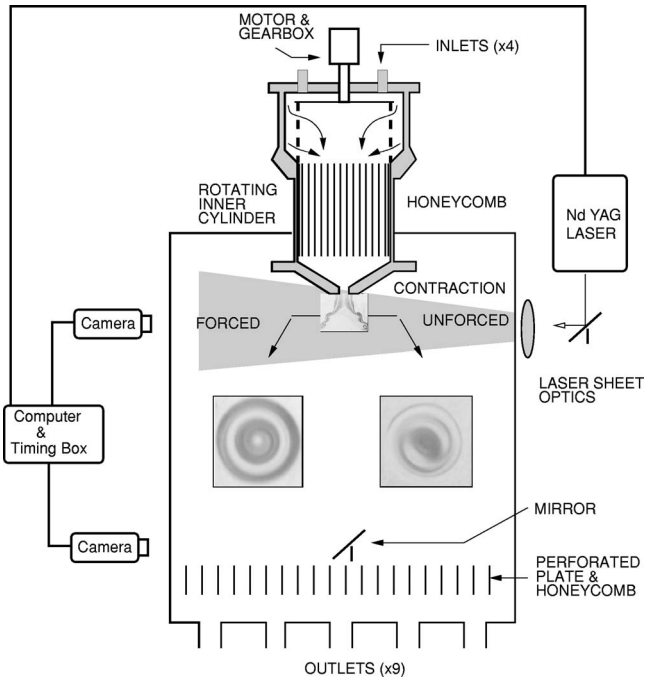

FIG. 1. The experimental setup. Note that the laser sheet is rotated for both horizontal and vertical plane cross sections. The insets show horizontal cross sections through the breakdown in the forced and unforced cases for Re=600 and $S=1.34$.

the cooler outflow over the warmer inflow via an intercooler core. In order to ensure slow-moving outlet flow, and to minimize pressure gradients caused by the outlet pipes, a perforated plate, acting as a honeycomb, is placed at the bottom of the test tank. This also had the advantage of retarding any whirlpool effect from occurring. Water consistency and temperature uniformity were vigilantly monitored with highly sensitive thermometers at specified locations around the whole circuit. The maximum temperature difference between the swirling jet and fluid within the test tank was found to be 0.5 °C.

In order to characterize this experiment, the following nondimensional variables were used. The swirl number S provides a measure for the ratio of azimuthal velocity U_θ to axial velocity U_z. Specifically,

$$S = \frac{U_{\theta\max}}{U_{z\max}} = \frac{2U_\theta(r=R/2)}{U_z(r=0)}.$$

At the critical swirl number, $S_c \simeq 1.3$, vortex breakdown is found to occur almost independent of the Reynolds number and nozzle diameter.[11] The Reynolds number characterizes the axial flow component, and is based on the jet diameter D and average axial velocity $\overline{U}_z$, which is extracted from the mean mass flow rate $\dot{m}$:

$$\mathrm{Re} = \frac{2R\overline{U}_z}{\nu}.$$

Here, ν is the kinematic viscosity. Furthermore, the Strouhal number nondimensionalizes the frequency of pulsing, f,

$$\mathrm{St} = \frac{2Rf}{\overline{U}_z}.$$

Finally, the sinusoidal variation in mass flow during pulsing is characterized by the relative amplitude of the velocity variation, which can be conveniently expressed in terms of mass flow rates as

$$\mathrm{A} = \frac{\dot{m}_{\max} - \overline{\dot{m}}}{\overline{\dot{m}}} = \frac{\overline{\dot{m}} - \dot{m}_{\min}}{\overline{\dot{m}}}.$$

Here, $\dot{m}_{\min}$ and $\dot{m}_{\max}$ are the minimum and maximum mass flow rates. For both visualization and particle image velocimetry (PIV) measurements, the water was seeded with spherical polyethylene (25 μm) particles with a specific gravity of 1.02. To create minimal disturbance to the flow, the particles were continuously fed into the flow as far upstream as possible. The injection rate was controlled via a piston-controlled injection chamber and a gravity-feed device. Particles were illuminated via a combination of stage lights and lasers. For PIV, the particles were illuminated using a laser sheet generated by a frequency-doubled Nd:YAG laser at 532 nm and 400 mJ in 5 ns bursts.

Flow visualizations were conducted using a 5 megapixel Minolta digital camera and a Kodak ES4 charge-coupled device (CCD) 4 megapixel camera, which was also used to acquire the raw PIV images. PIV was used for quantitative measurements of axial and swirl profiles in order to obtain the swirl number. PIV was performed using a cross-correlation-type analysis. Vorticity is calculated using a second-order least-squares fit in x and y (six terms) and then analytically differentiating this equation to obtain the derivatives.

For the unforced flow, nonaxisymmetric vortex breakdown is observed, closely analogous to that observed by Billant *et al.*[11] using a similar apparatus. A typical horizontal cross section through a *cone* breakdown for Re=600 and $S=1.34$ is shown as an inset in Fig. 1, revealing evidence of an $m=+2$ helical structure. Forcing significantly reduces the development of the asymmetry, as demonstrated by the other inset for the forced case. Here, the breakdown structure remains axisymmetric, at least for a considerable axial distance downstream of breakdown. At higher Reynolds numbers the suppression of nonaxisymmetry is less effective, with nonaxisymmetric flow apparent further upstream towards the breakdown stagnation point.

An examination of the (helical) vortex structures forming at the edge of the unforced swirling jet was conducted by using long exposure (0.5 s) images spanning a period of 120 s. A spectral analysis of the data revealed that the shear-layer Strouhal number is independent of the swirl number, in agreement with Loiseleux *et al.*[14] Furthermore, over the Reynolds number range tested, the Strouhal number is independent of Reynolds number to within 2 standard deviations of the mean and is fixed at $\mathrm{St}=\mathrm{St}_n=0.78\pm0.01$. The shear layer first sheds at approximately 1 to 2 nozzle diameters downstream in all cases, and appears to periodically shed in small bursts with durations and delays of the same order as the natural shedding frequency of the structure.

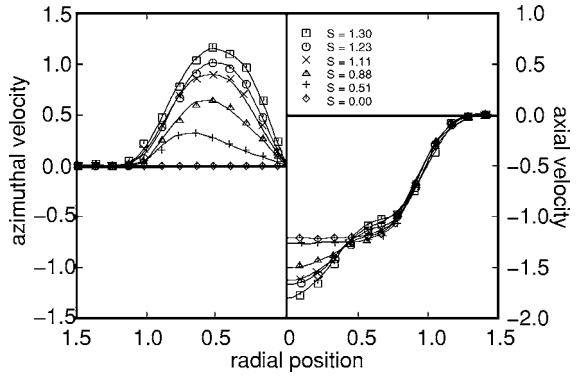

FIG. 2. Time-mean azimuthal and axial velocity profiles, respectively, generated from vertical plane PIV data at Re=900 and $z/R=0.7$.

Figure 2 shows measured axial and azimuthal velocity profiles as a function of radial position, for a series of swirl numbers. These profiles compare favorably to those obtained by Billant *et al.* (1999) using a similar experimental rig.

By sinusoidally pulsing the swirling jet mass flow rate $\dot{m}$, in the form $\dot{m}=\bar{\dot{m}}[1+\mathrm{A}\sin(2\pi ft)]$, it is possible to alter the vorticity structure within the shear layer, and to alter the vortex-shedding frequency. In fact, the shedding frequency of the swirling jet was found to lock onto forcing frequencies up to approximately twice the unpulsed or natural frequency of shedding. Above this critical value, the flow below the stagnation point where the shedding becomes apparent is unresponsive to the imposed perturbation and the jet sheds at its natural frequency independent of the amplitude of the perturbation. The shear layer is unreceptive when pulsing is conducted far from the natural frequency.

The effect of pulsing at various Strouhal numbers on breakdown was determined by flow visualization. The breakdown stagnation position z_B relative to the nozzle exit was found to increase, i.e., move further downstream, as the pulsing Strouhal number approached the natural Strouhal shedding frequency (see Fig. 3). This is in agreement with experiments conducted using delta wings.[10] To quantify this, it is useful to define the relative shift as $\zeta=(z_{Bp}-z_B)/z_B$, where z_{Bp} is the measured axial position of the breakdown when

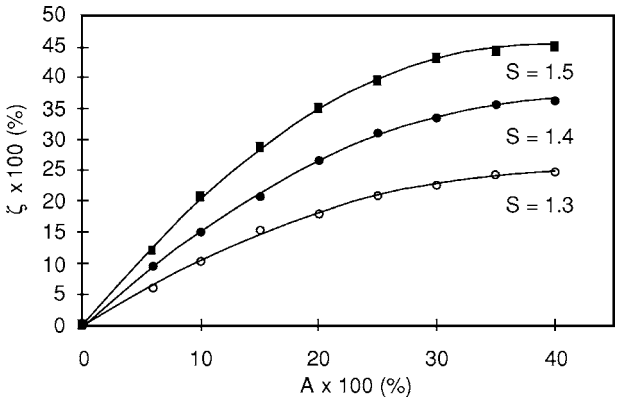

FIG. 3. Relative shift in breakdown position (ζ) as a function of relative perturbation amplitude (A) for different mean swirl ratios. Re=600. Similar results apply to other Reynolds numbers tested.

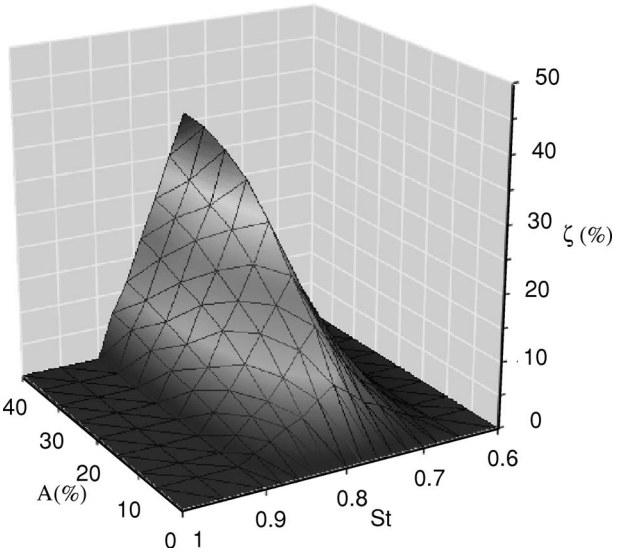

FIG. 4. Three-dimensional carpet plot representing the dependence of breakdown position (ζ) on forcing frequency (St) and perturbation amplitude (A) for $S=1.4$ and Re=600.

pulsing is applied. It was found that, to obtain significant downstream movement of the breakdown position, pulsing must be conducted at $\mathrm{St}=\mathrm{St}_n\pm10\%$. It needs to be noted that the present flow geometry produces a very robust form of vortex breakdown, due to the rapid and large expansion at the exit of the jet nozzle. The relative breakdowns observed here would be expected to translate to substantial movements of the breakdown position in situations where the flow gradients are less severe.

Some key findings are that axial pulsing within the hysteretic range at which breakdown exists has the ability to revert the core to the non-breakdown state, with perturbation amplitudes as low as 6–12%. An established breakdown moves downstream as perturbation amplitudes increase; however, the shift begins to saturate at $A>30$–40% (Fig. 4). For higher amplitudes, large fluctuations in the stagnation point position are observed on the order of 10%. Relative shifts of up to 50% occur at $S=S_c$ and St=0.78, with higher swirl stabilizing the structure, in agreement with Loiseleux *et al.*,[14] and lowering z_{Bp}. Flow visualizations and vorticity plots from PIV imaging at St=0.78 (Fig. 5) show that axial pulsing at this frequency causes the development of vortex (ring) structures within the shear layer and excites the shear-layer resonance.

The modifications to the shear-layer structure and the highly periodic shedding at $\mathrm{St}=0.78\pm10\%$ have the effect of forcing the stagnation point further downstream. From observations, it was also interesting to see that the stagnation point without pulsing was consistently further upstream than the axial position at which the shear layer begins to shed. However, when axial pulsing was applied at $\mathrm{St}=0.78\pm10\%$, the axial location at which shear-layer shedding began moved further upstream closer to the jet outlet consistently higher than the stagnation point, which moved downstream. PIV measurements indicate that, for the forced case upstream of breakdown, the mean axial velocity is increased on the centerline, while the mean swirl velocity profile is hardly af-

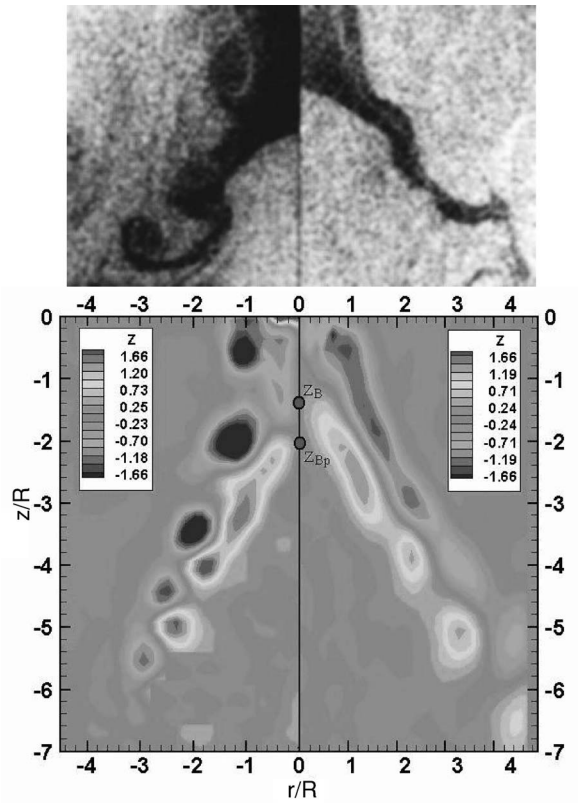

FIG. 5. Top: Instantaneous flow visualizations obtained using reflective particles and a laser sheet showing half of the jet. Flow is from top to bottom. Left: modification to breakdown under 30% axial forcing at $S=1.34$ for Re=600, St=0.78. Right: uncontrolled breakdown. Bottom: Gray scale vorticity contours obtained from PIV again for $S=1.34$ and Re=600, but for 25% forcing.

fected. Hence, forcing results in a lower mean swirl ratio, consistent with breakdown occurring further downstream. Quantitative details will appear elsewhere.

The following conclusions are drawn:

(1) For an unforced swirling jet, the Strouhal number of shear-layer vortex shedding is independent of Reynolds number and swirl number, and is fixed at $St=St_n=0.78$.
(2) For the forced case, the shedding frequency of the swirling jet was found to lock onto low frequencies up to approximately $2St_n$. Above this critical value, the flow below the stagnation point is not receptive to the higher frequency pulsing and the jet sheds at its natural frequency, independent of the amplitude of the forcing.
(3) To obtain significant downstream movement of the breakdown position, pulsing must be conducted close to the natural frequency, i.e., at $St=St_n\pm10\%$.
(4) Axial pulsing within the hysteretic range over which breakdown exists has the ability to destroy the breakdown structure altogether with perturbation amplitudes of only 6–12%. It is possible to shift the breakdown structure by up to 50% at $S=S_c$ and St=0.78.
(5) The growth and development of vortex ring structures within the shear layer and the highly periodic shedding at $St=0.78\pm10\%$ alters the mean axial velocity profile leading to a delay of breakdown.

We acknowledge support from Australian Research Council Discovery and LIEF grants, which enabled the experimental apparatus to be built. In addition, S.K. acknowledges scholarship support from an Australian Postgraduate Award.

[1] J. M. Delery, "Aspects of vortex breakdown," Prog. Aerosp. Sci. **30**, 1 (1994).
[2] O. Lucca-Negro and T. O'Doherty, "Vortex breakdown: A review," Prog. Energy Combust. Sci. **27**, 431 (2001).
[3] A. M. Mitchell and J. Delery, "Research into vortex breakdown control," Prog. Aerosp. Sci. **37**, 385 (2001).
[4] J. Er-El and A. Seginer, "Effects of spanwise blowing on pressure distribution and leading-edge vortex stability," in 15th Congress of the International Council of the Aeronautical Sciences, ICAS-86, London, England, 1986.
[5] D. B. Owens and J. Perkins, "Vortex suppression on highly-swept wings by suction boundary-layer control," in 33rd AIAA Aerospace Sciences Meeting and Exhibition, Reno, NV, 1995.
[6] P. V. Vorobieff and D. O. Rockwell, "Multiple-actuator control of vortex breakdown on a pitching delta wing," AIAA J. **34**, 2184 (1996).
[7] A. M. Mitchell, P. Molton, D. Barberis, and J. L. Gobert, "Control of vortex breakdown by along-the-core blowing," in AIAA Fluids 2000 Conference, Denver, CO, 2000.
[8] P. V. Vorobieff and D. O. Rockwell, "Vortex breakdown on pitching delta wing: control by intermittent trailing-edge blowing," AIAA J. **36**, 585 (1998).
[9] W. Gu, O. Robinson, and D. O. Rockwell, "Experimental study of vortex breakdown in swirling jets," AIAA J. **31**, 1177 (1993).
[10] W. Gu, O. Robinson, and D. O. Rockwell, "Delta wing vortex manipulation using pulsed and steady blowing during ramp-pitching," J. Aircr. **33**, 452 (1997).
[11] P. Billant, J. M. Chomaz, and P. Huerre, "Experimental study of vortex breakdown in swirling jets," J. Fluid Mech. **376**, 183 (1998).
[12] M. M. Wu, A. Garcia, J. M. Chomaz, and P. Huerre, "Instabilities in a swirling jet," Bull. Am. Phys. Soc. **7** (8), 1789 (1992).
[13] R. Wallis, *Axial Flow Fans and Ducts* (Wiley Interscience, New York, 1983).
[14] T. Loiseleux, J.-M. Chomaz, and P. Huerre, "Effect of swirl on jets and wakes: Linear instability of the Rankine vortex with axial flow," Phys. Fluids **10**, 1120 (1998).